Signal Reconstruction from a Periodic Nonuniform Set of Samples Using $\mathcal{H}_\infty$ Optimization

Ha T. Nguyen and Minh N. Do

Department of Electrical and Computer Engineering,
University of Illinois at Urbana Champaign *

ABSTRACT

We study the problem of signal reconstruction from a periodical nonuniform set of samples. The considered system takes samples of delayed versions of a continuous signal at low sampling rate, with different fractional delays for different channels. We design IIR synthesis filters so that the overall system approximates a sampling system of high sampling rate using techniques from model-matching problem in control theory with available software (such as Matlab). Unlike traditional signal processing methods, our approach uses techniques from control theory which convert systems with fractional delays into $\mathcal{H}$-norm-equivalent discrete-time systems. The synthesis filters are designed so that they minimize the $\mathcal{H}_\infty$ norm of the error system. As a consequence, the induced error is uniformly small over all (band-limited and band-unlimited) input signals. The experiments are also run for synthesized images.

Keywords: Super-resolution, model-matching, $\mathcal{H}_\infty$ optimization, polyphase, lifting, fractional delay, filter design, IIR filter.

1. INTRODUCTION

Hardware technologies show enormous advancements in recent years. These advancements drive the cost of measurement devices, such as digital cameras and sensors, to decrease considerably. As a result, in many applications such as image super-resolution,[2,6,7,15] sensor networks[1] and analog-to-digital converters,[20] one can use more and more measurement devices in the measurement process. Furthermore, more often than not, pushing the limit of hardware technologies is hard and expensive for a given application. An alternative is to use many low performance devices and an algorithm to fuse the data obtained from them.

A question that naturally arises from this context is how to exploit a large amount of data obtained from different measurement devices in an efficient way. In this paper, we address a concrete problem related to that question, that is to approximate a sampling device of high sampling rate using different low sampling rate ones.

Fig. 1 shows a high sampling rate system that we want to approximate. A continuous input signal $f(t) \in \mathcal{L}_2$ is convolved with a function whose Laplace transform is $\varphi(s)$. This convolution is a mathematical model of the effect of point-spread-function in optical measurement devices or the function governing the frequency response of inputs $f(t)$ as in analog-to-digital converters. The output of the convolution is then sampled at high sampling rate $h > 0$. The desired high resolution signal obtained by this system is denoted by $y[n]$.

Fig. 2 illustrates the system that we actually use to approximate the high sampling rate system in Fig. 1. The same continuous input signal $f(t) \in \mathcal{L}_2$ is convolved with the same function with Laplace transform $\varphi(s)$ before being delayed by d_1, d_2 at channel 1 and 2, for example because of traveling times of the signals. Low resolution signals $x_1[n], x_2[n]$ are taken at low rate $2h$ from delayed versions of the continuous signal $f(t)$.

The goal of the paper is to reconstruct the high resolution signal $y[n]$ of Fig. 1 using low resolution signals $x_1[n], x_2[n]$ of Fig. 2. Related problems have been addressed in literature. Herley and Wong[10] address the problem of sampling and reconstruction of periodic nonuniform samples under two assumptions: 1) that the input signals belong to a class of signals having fixed frequency support, and 2) the set of samples are the set left after discarding an uniform set of samples in a periodic fashion. Marziliano [14, Chapter 5] also address the problem of reconstructing a discrete signal from a periodic nonuniform set of samples using Fourier transform.

*This work was supported by the National Science Foundation under Grant ITR-0312432.

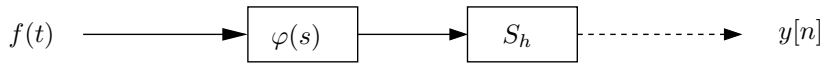

Figure 1. The high resolution signal $y[n]$ taken at high sampling rate h from the continuous signal $f(t)$.

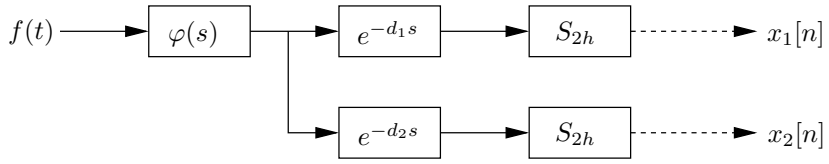

Figure 2. Low resolution signals $x_1[n], x_2[n]$ sampled at low rate $2h$ from delayed versions of the continuous signal $f(t)$. We want to reconstruct the high resolution signal $y[n]$ of Fig. 1 using low resolution signals $x_1[n], x_2[n]$.

However, the author only consider a limited set of input signals that are bandlimited. Jahromi and Aarabi[11] consider the problem of estimating the traveling times d_1, d_2, and of designing analysis and synthesis filters to minimize the $\mathcal{H}_\infty$-norm of the error system. The choice of $\mathcal{H}_\infty$ optimization makes the induced-l_2 norm of the approximation error uniformly small over all possible inputs. However, the authors only consider integer delays or approximation or fractional delays as IIR or FIR filters. Shu et. al.[17] address the problem of designing the synthesis filters for a filter banks to minimize the $\mathcal{H}_\infty$ norm of the induced error system. Their problem is similar to the problem considered in this paper, except that it does not consider the fractional delays but rational transfer function instead.

In this paper, we propose a method to design IIR and FIR synthesis filters which minimize the $\mathcal{H}_\infty$-norm of the induced error system. Unlike many traditional signal processing methods that follow l_2 optimization over some class of input signals $\mathcal{S} \in \mathcal{L}_2$, we propose to use the framework of $\mathcal{H}_\infty$ optimization.[8,9,17] As a consequence, the induced error is uniformly small over time while no assumption of the input signal $f(t) \in \mathcal{L}_2$ (such as band-limitedness) is necessary. Another contribution of the paper to the problem is to use techniques in control theory to convert systems with fractional delays into $\mathcal{H}_\infty$-norm equivalent discrete-time systems, hence enhance the results comparing to methods approximating the fractional delays by IIR or FIR filters.[12,16,21] A generalization of the paper will be presented in our journal version.

The remainder of this paper is organized as follows. Section 2 presents the problem formulation. In Section 3 we show that the original error system is equivalent to a finite-dimensional discrete-time system. Then in Section 4, we convert the problem further to a linear-time invariant problem. Section 5 presents the design procedure to design IIR synthesis filters. The conclusions are given in Section 6.

2. PROBLEM FORMULATION

We consider the system illustrated in Fig. 3. Note that the system is hybrid in the sense that it contains both continuous and discrete-time signals.

The input continuous signal $f(t) \in \mathcal{L}_2$ is convolved with a function whose Laplace transform is a rational function $\varphi(s)$. The output signal after the convolution then goes through three channels. In the first channel, the signal is sampled at high sampling rate h to get the high resolution measurement $y[n]$. In the second and third channels, the signal is delayed by $d_1, d_2 \in (0, h)$, and then sampled at low sampling rate $2h$ to get low resolution measurements $x_1[n], x_2[n]$. We want to design filters $F_1(z)$ and $F_2(z)$ to use $x_1[n], x_2[n]$ to reconstruct $\widehat{y}[n]$ – an approximation of $y[n]$ (tolerated by some delay tolerance of m samples) without any knowledge of the input $f(t)$. That is we want to design filters $F_1(z)$ and $F_2(z)$ based on the transfer function $\varphi(s)$, the delays d_1, d_2, the system delay tolerance m and the sampling rate h to minimize the $\mathcal{H}_\infty$-norm of the overall error system $\mathcal{E}$.

In the framework of $\mathcal{H}_\infty$ optimization, we work on the Hardy space $\mathcal{H}_\infty$ that consists of all complex value functions $G(s)$ of a complex variable s which are analytic and bounded in the open right haft-plane $\Re(s) > 0$. The $\mathcal{H}_\infty$-norm of $G(s)$ is defined as $\|G(s)\|_\infty = \sup\{|G(s)| : \Re(s) > 0\}$. If we consider $G(s)$ as the transfer function of some system with input $u(t)$, the $\mathcal{H}_\infty$-norm of $G(s)$ is $\|G(s)\|_\infty = \sup\{\|Gu\|_2 : \|u\|_2 \leq 1\}$.[8]

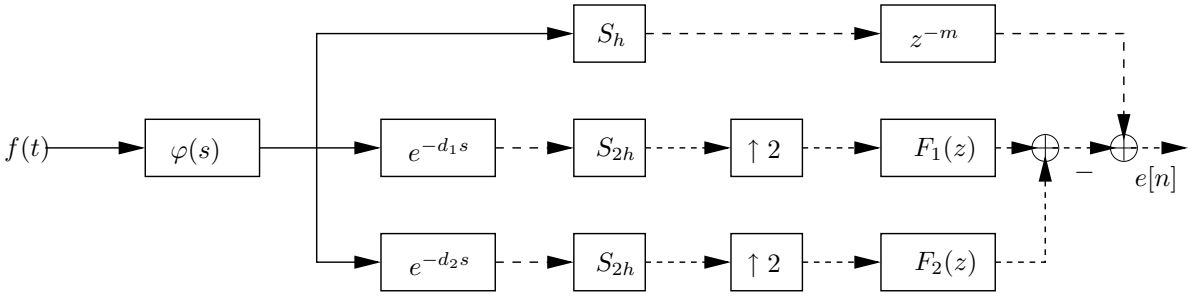

Figure 3. The error system $\mathcal{E}$. We want to design synthesis filters $F_1(z), F_2(z)$ based on the transfer function $\varphi(s)$, the sampling rate $h > 0$, the fractional delays $d_1, d_2 \in (0, h)$, and the system delay tolerance $m \geq 0$ to minimize the $\mathcal{H}_\infty$-norm of the overall error system $\mathcal{E}$.

In our problem, the $\mathcal{H}_\infty$-norm of the system $\mathcal{E}$ is defined as follows:

$$\|\mathcal{E}\|_\infty := \sup\{\|e\|_2 : \|f\|_2 \leq 1\}.$$

Problem 1:

- **Inputs:** transfer function $\varphi(s)$, the sampling rate $h > 0$, the delays $d_1, d_2 \in (0, h)$, and the delay tolerance $m \geq 0$.
- **Outputs:** synthesis filters $F_1(z), F_2(z)$.

Throughout the paper, we adopt the following conventions to clarify the presentation. An one dimensional signal $u(t)$ and a single-input single-output transfer function $G(s)$ is written in regular font, while a multi-dimensional signal $\mathbf{u}(t)$ and multi-input multi-output $\mathbf{G}(s)$ will be written in bold. In our figures, solid lines illustrate continuous signals, and dashed lines are intended for discrete ones. Furthermore, multi-dimensional signals will have bolder lines in our diagrams. Finally, when two systems are $\mathcal{H}_\infty$-norm equivalent, we will simply say that they are equivalent.

The paper uses some techniques of state-space methods. Readers who want to review in details can start at any textbook in control theory, for example.[3]

3. EQUIVALENCE OF $\mathcal{E}$ TO A FINITE-DIMENSIONAL DISCRETE-TIME SYSTEM

The error system $\mathcal{E}$ in Fig. 3 can be written as:

$$\begin{aligned}
\mathcal{E} &= (z^{-m})S_h\varphi(s) - F_1(z)(\uparrow 2)(\downarrow 2)S_h(e^{-d_1 s})\varphi(s) - F_2(z)(\uparrow 2)(\downarrow 2)S_h(e^{-d_2 s})\varphi(s) \\
&= \underbrace{\begin{bmatrix} z^{-m} & -F_1(z)(\uparrow 2)(\downarrow 2) & -F_2(z)(\uparrow 2)(\downarrow 2) \end{bmatrix}}_{\mathbf{F}_d} \underbrace{\begin{bmatrix} S_h & 0 & 0 \\ 0 & S_h & 0 \\ 0 & 0 & S_h \end{bmatrix}}_{\mathbf{S}_h} \underbrace{\begin{bmatrix} \varphi(s) \\ e^{-d_1 s}\varphi(s) \\ e^{-d_2 s}\varphi(s) \end{bmatrix}}_{\mathbf{G}_c}.
\end{aligned}$$

Hence the system $\mathcal{E}$ can be considered as a cascade of three systems:

$$\mathcal{E} = \mathbf{F}_d \mathbf{S}_h \mathbf{G}_c, \tag{1}$$

in which $\mathbf{G}_c(s)$ is an one-input three-output continuous-time system; $\mathbf{S}_h$ is the sampling operator – in this case all 3 channels are sampled at the same sampling rate h; and $\mathbf{F}_d(z)$ is a finite-dimensional discrete-time system to be design. In this section, we want to show that there exists a finite-dimensional discrete-time system that has the same $\mathcal{H}_\infty$-norm with our original error system $\mathcal{E}$. This can be done if the first part $\mathbf{S}_h\mathbf{G}_c$ of $\mathcal{E}$ (Fig. 4) can be shown $\mathcal{H}_\infty$-norm equivalent to a finite-dimensional discrete-time system. We show that in two steps. In the first step (Section 3.1), we convert the original system into a discrete-time system. However, this system will be of infinite-dimensional. In the second step (section 3.2), we convert the infinite-dimensional problem into a finite-dimensional one.

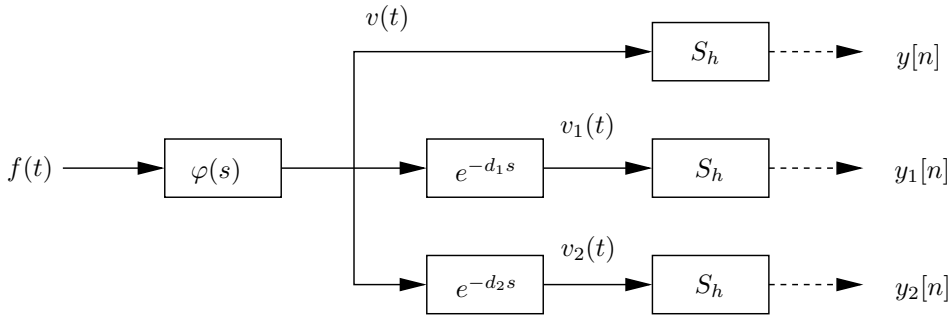

Figure 4. The continuous to discrete conversion part $\mathbf{S}_h\mathbf{G}_c$ of the error system $\mathcal{E}$. Note that the sampling rate of all three channels is h. Hence $x_1[n], x_2[n]$ in Fig. 2 are downsampled-by-2 version of $y_1[n], y_2[n]$, respectively.

3.1. Equivalence of $\mathcal{E}$ to discrete-time system

We first define the lifting operator $\mathcal{L}_h$ as follows.

Definition 3.1 (The lifting operator $\mathcal{L}_h$). *[4, Section 10.1] The lifting operator $\mathcal{L}_h$ takes a continuous-time signal $u(t)$ as input and output a discrete-time signal $\{\widetilde{u}[n]\}_{n\in\mathbb{Z}}$:*

$$\widetilde{u} = \mathcal{L}_h(u) = \Big[\dots, \widetilde{u}[-1], \widetilde{u}[0], \widetilde{u}[1], \widetilde{u}[2], \dots\Big]^T,$$

in which:

$$(\widetilde{u}[n])(t) := u(nh+t)|_{0\le t<h} \in \mathcal{K} := L_2[0,h).$$

Remark 1. *The lifting operator $\mathcal{L}_h$ preserves the energy of the signal, i.e.:*

$$\|u(t)\|_2 = \|\widetilde{u}[n]\|_2.$$

Let us now consider the subsystem $\mathbf{S}_h\mathbf{G}_c$ as in Fig. 4. Suppose that $[A, B, C, 0]$ is a realization of $\varphi(s)$ with state function $x(t)$, that is:

$$\begin{cases} \dot{x}(t) &= Ax(t) + Bf(t) \\ v(t) &= Cx(t). \end{cases}$$

For $0 < t_1 < t_2 < \infty$, we can compute the future state value $x(t_2)$ from a previous one $x(t_1)$ as follows:

$$x(t_2) = e^{(t_2-t_1)A}x(t_1) + \int_{t_1}^{t_2} e^{(t_2-\tau)A}Bf(\tau)d\tau. \tag{2}$$

We define linear operators $\mathbf{B}_0, \mathbf{B}_1$ and $\mathbf{B}_2$ taking inputs $u(t) \in \mathcal{K}$ as follows:

$$\begin{aligned} \mathbf{B}_0 u &= \int_0^h e^{(h-\tau)A}Bu(\tau)d\tau \\ \mathbf{B}_i u &= C\int_0^{h-d_i} e^{(h-d_i-\tau)A}Bu(\tau)d\tau, \quad i = 1, 2. \end{aligned}$$

Applying Eq. (2) using $t_1 = nh$ and $t_2 = (n+1)h$ we get:

$$\begin{aligned} x((n+1)h) &= e^{hA}x(nh) + \int_{nh}^{(n+1)h} e^{((n+1)h-\tau)A}Bf(\tau)d\tau \\ &= e^{hA}x(nh) + \mathbf{B}_0\widetilde{f}[n]. \end{aligned}$$

Similarly, applying Eq. (2) with $t_1 = nh$ and $t_2 = (n+1)h - d_i$, for $i = 1, 2$, we get:

$$\begin{aligned} x((n+1)h - d_i) &= e^{(h-d_i)A}x(nh) + \int_{nh}^{(n+1)h-d_i} e^{((n+1)h-d_i-\tau)A}Bf(\tau)d\tau \\ \Longrightarrow \quad v_i((n+1)h) &= Cx((n+1)h - d_i) \\ &= Ce^{(h-d_i)A}x(nh) + \mathbf{B}_i\widetilde{f}[n]. \end{aligned}$$

Let $x_d[n] = [x(nh), v_1(nh), v_2(nh)]^T$, then we obtain the discrete-time system from input $\widetilde{f}[n] = \mathcal{L}_h\big(f(t)\big)$ to output $\big[y[n], y_1[n], y_2[n]\big]^T = \big[v(nh), v_1(nh), v_2(nh)\big]^T$ as:

$$x_d[n+1] = \underbrace{\begin{bmatrix} e^{hA} & 0 & 0 \\ Ce^{(h-d_1)A} & 0 & 0 \\ Ce^{(h-d_2)A} & 0 & 0 \end{bmatrix}}_{A_d} x_d[n] + \underbrace{\begin{bmatrix} \mathbf{B}_0 \\ \mathbf{B}_1 \\ \mathbf{B}_2 \end{bmatrix}}_{\mathbf{B}_{id}} \widetilde{f}[n] \tag{3}$$

$$\begin{bmatrix} y[n] \\ y_1[n] \\ y_2[n] \end{bmatrix} = \underbrace{\begin{bmatrix} C & 0 & 0 \\ 0 & 1 & 0 \\ 0 & 0 & 1 \end{bmatrix}}_{C_d} x_d[n]. \tag{4}$$

The system $\mathbf{S}_h\mathbf{G}_c$ is hence equivalent to the infinite-dimensional discrete-time system

$$\mathbf{G}_{id} = [A_d, \mathbf{B}_{id}, C_d, 0].$$

3.2. Equivalence of $\mathcal{E}$ to finite-dimensional discrete-time system

The next step is to convert this infinite-dimensional discrete system $\mathbf{G}_{id}$ into some finite-dimensional discrete-time system $\mathbf{G}_d$. We define adjoint operators $\mathbf{B}_0^*, \mathbf{B}_1^*, \mathbf{B}_2^*$ of $\mathbf{B}_0, \mathbf{B}_1, \mathbf{B}_2$ respectively as follows:

$$\begin{aligned} (\mathbf{B}_0^* x)(t) &= B^T e^{(h-t)A^T} x, \\ (\mathbf{B}_i^* x)(t) &= \mathbf{1}_{[0,h-d_i)} B^T e^{(h-d_i-t)A^T} C^T x, \quad i = 1, 2. \end{aligned}$$

Hence, the adjoint operator of $\mathbf{B}_{id} = [\mathbf{B}_0 \quad \mathbf{B}_1 \quad \mathbf{B}_2]^T$ is $\mathbf{B}_{id}^* = [\mathbf{B}_0^* \quad \mathbf{B}_1^* \quad \mathbf{B}_2^*]$. Lemma 3.2 provides a formula to compute the norm of $\mathbf{B}_{id}$.

LEMMA 3.2. *The linear operator $\Sigma = \boldsymbol{B}_{id}\boldsymbol{B}_{id}^*$ is characterized by the following matrix:*

$$\Sigma = \begin{bmatrix} M(h) & e^{d_1 A}M(h-d_1)C^T & e^{d_2 A}M(h-d_2)C^T \\ CM(h-d_1)e^{d_1 A^T} & CM(h-d_1)C^T & \Sigma_{12} \\ CM(h-d_2)e^{d_2 A^T} & \Sigma_{12}^T & CM(h-d_2)C^T \end{bmatrix},$$

in which

$$\begin{aligned} \Sigma_{12} &= Ce^{(\max\{d_1,d_2\}-d_1)A}M(h - \max\{d_1, d_2\})e^{(\max\{d_1,d_2\}-d_2)A^T}C^T \\ M(t) &:= \int_0^t e^{\tau A}BB^T e^{\tau A^T} d\tau. \end{aligned}$$

REMARK 2. *$M(t)$ can be efficiently computed as:*[13]

$$\begin{aligned} M(t) &= F_{22}^T(t)F_{12}(t), \\ \begin{bmatrix} F_{11}(t) & F_{12}(t) \\ 0 & F_{22}(t) \end{bmatrix} &:= \exp\left(\begin{bmatrix} -A & BB^T \\ 0 & A^T \end{bmatrix} t\right). \end{aligned}$$

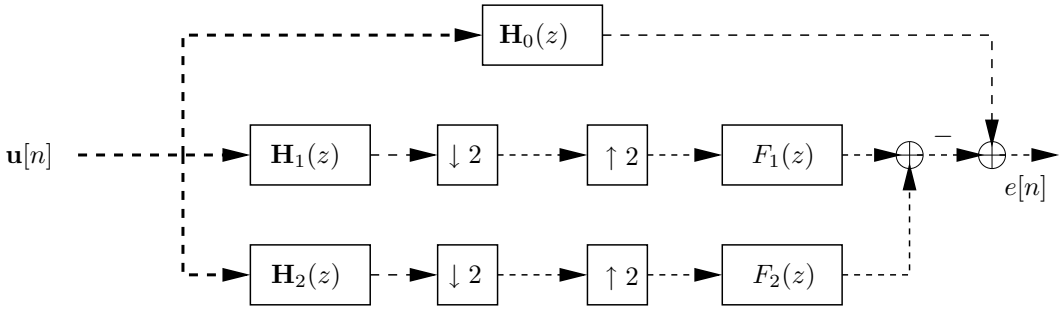

Figure 5. The $\mathcal{H}_\infty$-norm equivalent discrete-time system $\mathcal{E}_d$ of the original hybrid error system $\mathcal{E}$. Here $\mathbf{H}_i(z), (i = 0, 1, 2)$, are rational transfer functions defined in Eq. (6). The input $\mathbf{u}[n]$ is a multiple dimensional signal.

The Matlab command `expm` *can be used to numerically compute the exponential of a matrix.*

Note that although $\mathbf{B}_{id}$ has infinite columns, the matrix $\mathbf{B}_{id}\mathbf{B}_{id}^*$ is a square matrix of finite dimension. Hence we can find some square root matrix B_d of $\mathbf{B}_{id}\mathbf{B}_{id}^*$, that is B_d satisfying:

$$B_d B_d^* = \mathbf{B}_{id}\mathbf{B}_{id}^*. \tag{5}$$

A simple Matlab command `sqrtm` does this trick. The matrix B_d can also be any Choleski matrix of $\mathbf{B}_{id}\mathbf{B}_{id}^*$ (using the Matlab command `chol`).

We have Proposition 1 proving that the finite-dimensional discrete-time system $\mathbf{G}_d(z) = [A_d, B_d, C_d, 0]$ is equivalent to the continuous part $\mathbf{S}_h\mathbf{G}_c$ of $\mathcal{E}$.

PROPOSITION 1. *The discrete-time system $\boldsymbol{G}_d(z) = [A_d, B_d, C_d, 0]$ has the same $\mathcal{H}_\infty$-norm with $\boldsymbol{S}_h\boldsymbol{G}_c$:*

$$\|\boldsymbol{G}_d\|_\infty = \|S_h G_c\|_\infty.$$

Proof. See [4, Section 10.5]. □

The system $\mathbf{G}_d(z) = [A_d, B_d, C_d, 0]$ is a discrete-time equivalence of the continuous part $\mathbf{S}_h\mathbf{G}_c$ in Eq. (1). In the following, we will derive a the discrete-time system equivalence $\mathcal{E}_d$ of the original hybrid system $\mathcal{E}$.

We observe that the matrix C_d in Eq. (4) has three rows. Let $C_d = [C_0, C_1, C_2]^T$. We also denote $[A_i, B_i, C_i, 0]$ a state-space realization of $\mathbf{H}_i(z)$ for $i = 0, 1, 2$. (It can be easily verified that the D-matrices of $\mathbf{H}_i(z)$ are 0 for $i = 0, 1, 2$). Thus:

$$\begin{array}{lll} \mathbf{H}_0(z) & = [A_0, B_0, C_0, 0] & = z^{-m}C_0(zI - A_d)^{-1}B_d \\ \mathbf{H}_i(z) & = [A_d, B_d, C_i, 0] & = C_i(zI - A_d)^{-1}B_d, \quad i = 1, 2. \end{array} \tag{6}$$

Hence $\mathbf{H}_i(z), (i = 0, 1, 2)$, are rational transfer functions taking multiple inputs. The error system $\mathcal{E}$ is equivalent to the multi-input one-output discrete-time system $\mathcal{E}_d(z)$ illustrated in Fig. 5.

4. EQUIVALENCE OF $\mathcal{E}$ TO A LINEAR TIME INVARIANT SYSTEM

The system $\mathcal{E}_d$ in Fig. 5 is discrete-time, but it is not linear time invariant (LTI) because of the presence of multirate operators $(\uparrow 2), (\downarrow 2)$. In this section, we want to modify $\mathcal{E}_d$ to an equivalent system that is LTI by using polyphase techniques.[18,19] Readers are referred to[17] for another technique to modify $\mathcal{E}$ to an LTI system.

We introduce polyphase matrices $\mathbf{Q}(z)$ and $\mathbf{K}(z)$ for analysis filters $\mathbf{H}_1(z), \mathbf{H}_2(z)$ and synthesis filters $F_1(z), F_2(z)$, and polyphase components $\mathbf{H}_{00}(z), \mathbf{H}_{01}(z)$ of $\mathbf{H}_0(z)$ as:

$$\begin{aligned} \begin{bmatrix} \mathbf{H}_1(z) \\ \mathbf{H}_2(z) \end{bmatrix} &= \mathbf{Q}(z^2) \begin{bmatrix} I \\ zI \end{bmatrix} \\ [F_1(z) \quad F_2(z)] &= [1 \quad z^{-1}]\, \mathbf{K}(z^2) \\ \mathbf{H}_0(z) &= \left[\mathbf{H}_{00}(z^2) \quad \mathbf{H}_{01}(z^2)\right] \begin{bmatrix} I \\ zI \end{bmatrix}, \end{aligned}$$

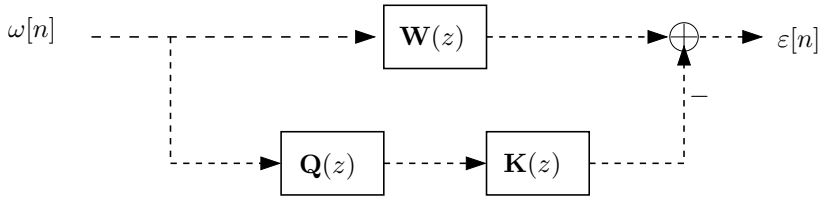

Figure 6. The equivalent LTI error system. Note that the system is multi-inputs (say of dimension N) two outputs ($\omega[n] \in \mathbb{R}^N, \varepsilon[n] \in \mathbb{R}^2$), the transfer matrices $\mathbf{W}(z), \mathbf{Q}(z)$ are of dimension $2 \times 2N$, and $\mathbf{K}(z)$ is 2×2.

in which I is the identity (square) matrix having the same number of rows as B_d. The discrete error system $\mathcal{E}_d$ can be described as:

$$\begin{aligned}
\mathcal{E}_d &= \mathbf{H}_0(z) - [F_1(z) \quad F_2(z)] \begin{bmatrix} (\uparrow 2) & 0 \\ 0 & (\uparrow 2) \end{bmatrix} \begin{bmatrix} (\downarrow 2) & 0 \\ 0 & (\downarrow 2) \end{bmatrix} \begin{bmatrix} \mathbf{H}_1(z) \\ \mathbf{H}_2(z) \end{bmatrix} \\
&= \begin{bmatrix} (\uparrow 2) & z^{-1}(\uparrow 2) \end{bmatrix} \left\{ \begin{bmatrix} \mathbf{H}_{00}(z) & \mathbf{H}_{01}(z) \\ z\mathbf{H}_{01}(z) & \mathbf{H}_{00}(z) \end{bmatrix} - \mathbf{K}(z)\, \mathbf{Q}(z) \right\} \begin{bmatrix} (\downarrow 2)I \\ (\downarrow 2)zI \end{bmatrix}.
\end{aligned}$$

Since operators $\begin{bmatrix} (\uparrow 2) & z^{-1}(\uparrow 2) \end{bmatrix}$ and $\begin{bmatrix} (\downarrow 2)I \\ (\downarrow 2)zI \end{bmatrix}$ are both norm-preserving on l_2, we can conclude that:

$$\|\mathcal{E}_d\|_\infty = \|\mathbf{W}(z) - \mathbf{K}(z)\mathbf{Q}(z)\|_\infty,$$

in which:

$$\mathbf{W}(z) = \begin{bmatrix} \mathbf{H}_{00}(z) & \mathbf{H}_{01}(z) \\ z\mathbf{H}_{01}(z) & \mathbf{H}_{00}(z) \end{bmatrix}. \tag{7}$$

Fig. 6 shows the equivalent discrete-time, LTI error system. The state-space realizations of $\mathbf{Q}(z)$ and $\mathbf{W}(z)$ are given in Proposition 2.

PROPOSITION 2. *The original error system $\mathcal{E}$ has an $\mathcal{H}_\infty$-norm equivalent discrete-time, LTI error system as shown in Fig. 6:*

$$\|\mathcal{E}\|_\infty = \|\, \boldsymbol{W}(z) - \boldsymbol{K}(z)\, \boldsymbol{Q}(z)\|_\infty, \tag{8}$$

in which $\boldsymbol{Q}(z)$ is the polyphase representation of analysis filters $\boldsymbol{H}_1(z), \boldsymbol{H}_2(z)$, and $\boldsymbol{W}(z)$ is given in Eq. (7). The state-space realizations of $\boldsymbol{Q}(z)$ and $\boldsymbol{W}(z)$ are given by:

$$\boldsymbol{Q}(z) := \left[\begin{array}{c|c} A_q & B_q \\ \hline C_q & D_q \end{array}\right] = \left[\begin{array}{c|cc} A_d^2 & A_dB_d & B_d \\ \hline C_1 & 0 & 0 \\ C_2 & 0 & 0 \end{array}\right], \tag{9}$$

$$\boldsymbol{W}(z) := \left[\begin{array}{c|c} A_w & B_w \\ \hline C_w & D_w \end{array}\right] = \left[\begin{array}{c|cc} A_0^2 & A_0B_0 & B_0 \\ \hline C_0 & 0 & 0 \\ C_0A_0 & C_0B_0 & 0 \end{array}\right] \tag{10}$$

Proof. See[17] for the proof of a similar proposition. □

5. DESIGN OF IIR FILTERS

Designing $\mathbf{K}(z)$ to minimize the $\mathcal{H}_\infty$ norm of the system $[\mathbf{W}(z) - \mathbf{K}(z)\mathbf{Q}(z)]$ is a standard problem in $\mathcal{H}_\infty$ optimization.[8,9,17] The solutions to the problem has existing software, such as Matlab's Robust Control Toolbox,[5] to facilitate the optimization process. The key command in Matlab to find the synthesis system $\mathbf{K}(z)$ is `hinfsyn`. Note that this command operates in continuous-time domain, hence we need to convert the discrete-time $\mathcal{H}_\infty$ problem into a continuous-time one using bilinear transformation.[4]

We note furthermore that the $\mathcal{H}_\infty$ optimization tool in Matlab uses the form described in Fig. 7. The system $\mathbf{P}(z)$ is computed based on $\mathbf{W}(z)$ and $\mathbf{Q}(z)$ as in Step 5 in the design procedure subsequently outlined.

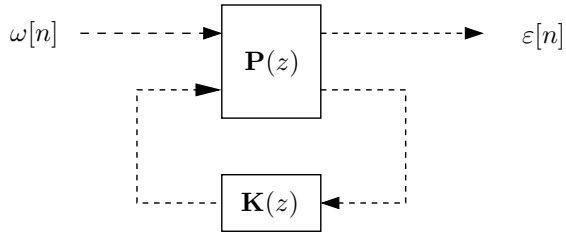

Figure 7. The final error model $E(z)$ (from $\omega[n]$ to $\varepsilon[n]$) used to design synthesis system $\mathbf{K}(z)$.

5.1. Design Procedure

- **Inputs:** Transfer function $\varphi(s)$, the delays $d_1, d_2 > 0$, the delay tolerance $m \geq 0$ and the sampling rate $h > 0$.
- **Outputs:** Synthesis IIR filters $F_1(z), F_2(z)$.

1. Compute a state-space realization $[A, B, C, 0]$ of $\varphi(s)$.
2. Compute the system $\mathbf{G}_d = [A_d, B_d, C_d, 0]$ as in Eq. (3), (4), (5).
3. Compute a state-space realization of $\mathbf{H}_i(z)$ as in Eq. (6) for $i = 0, 1, 2$.
4. Compute the state-space realization of $\mathbf{Q}(z)$ and $\mathbf{W}(z)$ as in Eq. (9) and in Eq. (10).
5. Compute the state-space realization of $\mathbf{P}(z)$ from $\mathbf{Q}(z)$ and $\mathbf{W}(z)$:

$$\mathbf{P}(z) := \left[\begin{array}{c|c} A_p & B_p \\ \hline C_p & D_p \end{array}\right] = \left[\begin{array}{cc|cc} A_w & 0 & B_w & 0 \\ 0 & A_q & B_q & 0 \\ \hline C_w & 0 & D_w & -I \\ 0 & C_q & D_q & 0 \end{array}\right]. \tag{11}$$

6. Design system $\mathbf{K}(z)$ to minimize the $\mathcal{H}_\infty$ norm of the system from $\omega[n]$ to $\varepsilon[n]$ in Fig. 7.
7. Obtain $F_1(z), F_2(z)$ from $\mathbf{K}(z)$ by:

$$[F_1(z) \quad F_2(z)] = [1 \quad z^{-1}]\, \mathbf{K}(z^2). \tag{12}$$

5.2. Experimental results

We present the experimental results for the following setting:

- The point spread function $\varphi(s) = \omega_c^2/(s + \omega_c)^2$, for $\omega_c = 0.5$.
- A step function as input: $f(t) = f_\tau(t) = \begin{cases} 0, & t < \tau \\ 1, & t \geq \tau \end{cases}$
- $m = 10, \quad h = 1, \quad d_1 = 0.2, \quad d_2 = 0.6.$

Fig. 8 shows the magnitude and phase response of synthesized filters $F_1(z)$ (dashed), and $F_2(z)$ (solid). It is quite interesting to note that the synthesized filters are nearly linear phase.

In Fig. 9, we plot the error $e[n]$ (solid) against the desired output $y[n]$ (dashed) with input $f(t)$. Note that the system is designed without any knowledge nor assumption (such as bandlimitedness) on the input signals (in this case, the step function $f(t)$ is not bandlimited). We can see that the error is small compared to the desired output $y[n]$. The $\mathcal{H}_\infty$-norm of the system is $\|\mathcal{E}\|_\infty \approx 3.33\%$.

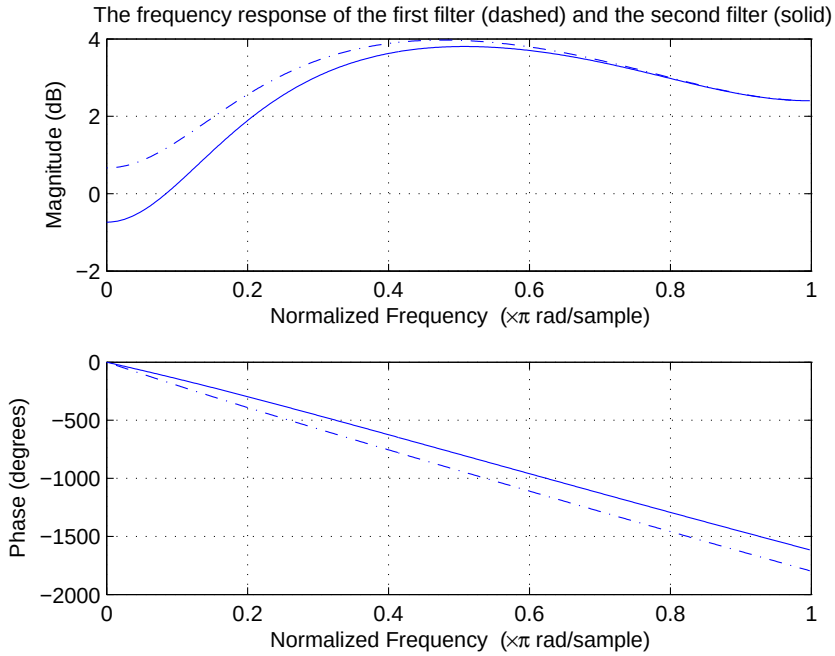

Figure 8. The magnitude and phase response of synthesized filters $F_1(z)$ (dashed), and $F_2(z)$ (solid).

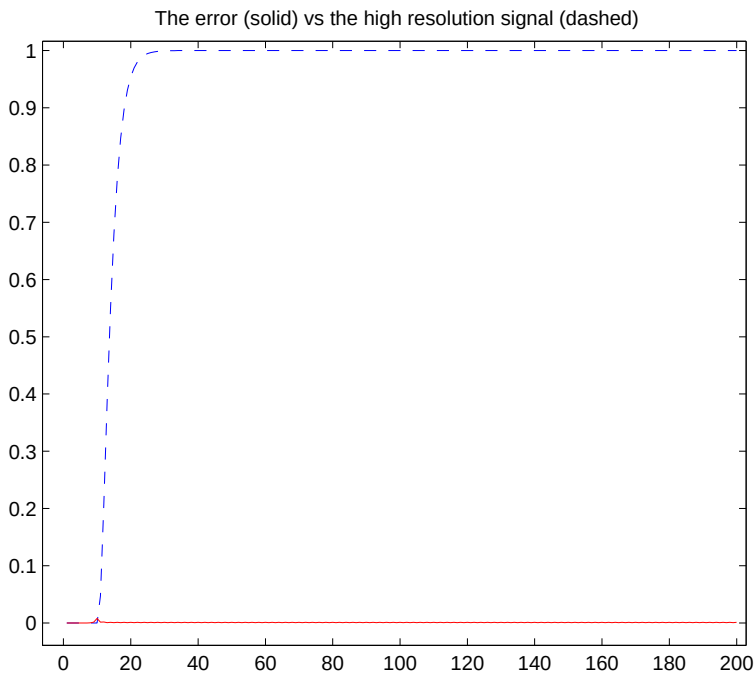

Figure 9. The error $e[n]$ (solid) plotted against the desired output $y[n]$ (dashed). The input $f(t)$ is a step function. The $\mathcal{H}_\infty$-norm of the system is $\|\mathcal{E}\|_\infty \approx 3.33\%$.

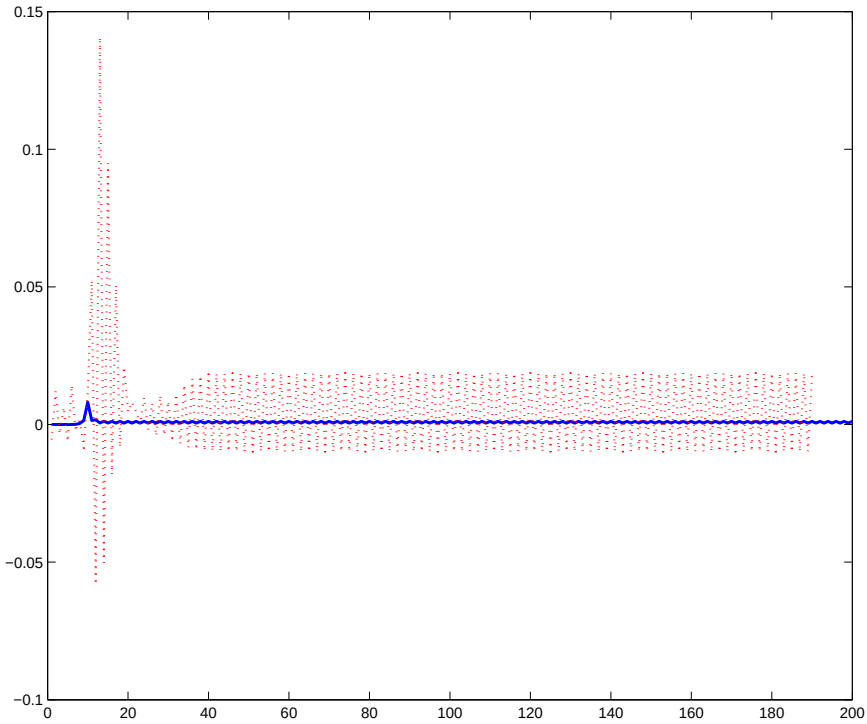

Figure 10. Comparison of the error of the proposed method (solid line) and the error of a traditional technique using the *sinc* function and interleaving (dotted line). We can see that the proposed method outperforms the traditional method, especially around the discontinuities.

Fig. 10 shows a comparison of the error of the proposed method (solid line) and the error of a traditional method using the *sinc* function for each channel separately and then interleaving the channels altogether (dotted line). We can see that the proposed method outperforms the traditional method, especially around the discontinuities where energy of high frequencies reside. Measurements confirm our observation: the proposed method outperforms the traditional one (with l_2 norm 0.0011 and 0.0201, respectively).

5.3. Application to images

We apply the proposed design method to a special case of the image superresolution problem in a separable fashion. Suppose that we want to approximate the desired high resolution image $y[m,n] = (f * \varphi)(mh, nh)$ using 4 low resolution images $y_{ij}[m,n] = (f * \varphi)(2mh + dx_i, 2nh + dy_j), i, j = 1, 2$. In our paper we use the same $\varphi(s)$ as in Section 5.2 and $h = 1, dx_1 = 0.3, dx_2 = 0.7, dy_1 = 0.4, dy_2 = 0.6$.

Fig. 11 shows the reconstructed image $\widehat{y}[m,n]$ compared to the desired image $y[m,n]$. The SNR of the reconstructed image $\widehat{y}[m,n]$ is about 43.95 dB. We can see the advantage of using $\mathcal{H}_\infty$ optimization: the reconstruction errors are small even with inputs having high frequency components, that enhances the visual quality of the reconstructed images.

6. CONCLUSIONS

We present a technique to reconstruct a signal from a periodic nonuniform set of samples. Unlike many traditional signal processing methods, we propose to minimize the $\mathcal{H}_\infty$-norm of the error system. As a consequence, the induced error is uniformly small over all (band-limited or band-unlimited) input signals $f(t) \in \mathcal{L}_2$. Moreover,

the proposed method uses techniques in control theory to find for systems with fractional delays $\mathcal{H}_\infty$-norm equivalent discrete-time systems. Hence, the proposed method enhances the results comparing to traditional methods approximating fractional delays using IIR or FIR filters.

A generalization of the method presented in this paper will be submitted for publication in the near future.

7. ACKNOWLEDGEMENTS

The authors are grateful to Linh Vu and Myra Nam (Department of Electrical and Computer Engineering, University of Illinois at Urbana Champaign) for useful discussion.

REFERENCES

1. I. Akyildiz, W. Su, Y. Sankarasubramaniam, and E. Cayirci, "A survey on sensor networks," *IEEE Communications Magazine*, vol. 40, no. 8, pp. 102–114, August 2002.
2. S. Baker and T. Kanade, "Limits on super-resolution and how to break them," *IEEE Trans. Patt. Recog. and Mach. Intell.*, vol. 24, no. 9, pp. 1167–1183, September 2002.
3. C.-T. Chen, *Linear System Theory and Design*, 3rd ed. Oxford University Press, 1999.
4. T. Chen and B. Francis, *Optimal Sampled-Data Control Systems.* Springer, 1995.
5. R. Y. Chiang and M. G. Safonov, "MATLAB - robust control toolbox," `http://www.mathworks.com`, 2005.
6. M. Elad and A. Feuer, "Super-resolution reconstruction of image sequences," *IEEE Trans. Patt. Recog. and Mach. Intell.*, vol. 21, no. 9, pp. 817–834, September 1999.
7. S. Farsiu, M. D. Robinson, M. Elad, and P. Milanfar, "Advances and challenges in super-resolution," *International Journal of Imaging Systems and Technology, Special Issue on High Resolution Image Reconstruction*, vol. 14, no. 2, pp. 47–57, August 2004.
8. B. Francis, *A Course in $\mathcal{H}_\infty$ Control Theory.* Springer-Verlag, 1987.
9. M. Green and D. J. N. Limebeer, *Linear Robust Control.* Upper Saddle River, NJ, USA: Prentice-Hall, Inc., 1995.
10. C. Herley and P. W. Wong, "Minimum rate sampling and reconstruction of signals with arbitrary frequency support," *IEEE Trans. Info. Theory*, vol. 45, no. 5, pp. 1555–1564, July 1999.
11. O. S. Jahromi and P. Aarabi, "Theory and design of multirate sensor arrays," *IEEE Trans. Signal Proc.*, vol. 53, no. 5, May 2005.
12. J. Lam, "Model reduction of delay systems using Pade approximation," *International Journal of Control*, vol. 57, no. 2, pp. 377–391, 1993.
13. C. F. V. Loan, "Computing integrals involving the matrix exponential," *IEEE Trans. Autom. Control*, vol. 23, no. 3, pp. 395–404, June 1978.
14. P. Marziliano, "Sampling inovations," Ph.D. dissertation, Ecole Polytechnique Federale de Lausanne, 2001.
15. S. C. Park, M. K. Park, and M. G. Kang, "Super-resolution image reconstruction: a technical overview," *IEEE Signal Proc. Mag.*, vol. 20, no. 3, pp. 21–36, May 2003.
16. L. D. Philipp, A. Mahmood, and B. L. Philipp, "An improved refinable rational approximation to the ideal time delay," *IEEE Trans. Circ. and Syst.*, vol. 46, no. 5, pp. 637–640, May 1999.
17. H. Shu, T. Chen, and B. Francis, "Minimax design of hybrid multirate filter banks," *IEEE Trans. Circ. and Syst.*, vol. 44, no. 2, February 1997.
18. P. P. Vaidyanathan, *Multirate Systems and Filter Banks.* Prentice Hall, 1993.
19. M. Vetterli and J. Kovačević, *Wavelets and Subband Coding.* Prentice-Hall, 1995.
20. R. H. Walden, "Analog-to-digital converter survey and analysis," *IEEE Journ. on Sel. Areas in Commun.*, vol. 17, no. 4, pp. 539–550, April 1999.
21. M. G. Yoon and B. H. Lee, "A new approximation method for time-delay systems," *IEEE Trans. Autom. Control*, vol. 42, no. 7, pp. 1008–1012, July 1997.

(a) The desired image

(b) The reconstructed image

Figure 11. The desired image $y[m,n]$ (a) and the reconstructed image $\widehat{y}[m,n]$ (b). $SNR \approx 43.95\ dB$. We can see the advantage of using $\mathcal{H}_\infty$ optimization: the reconstruction errors are small even with inputs having high frequency components, that enhances the visual quality of the reconstructed images.